water

MDPI

Article

Interactive Changes in Climatic and Hydrological Droughts, Water Quality, and Land Use/Cover of Tajan Watershed, Northern Iran

Mohammadtaghi Avand [1], Hamid Reza Moradi [1] and Zeinab Hazbavi [2,*]

[1] Department of Watershed Science and Engineering, Faculty of Natural Resources and Marine Sciences, Tarbiat Modares University, Noor 46417-76489, Mazandaran, Iran; mt.avand70@gmail.com (M.A.); hrmoradi@modares.ac.ir (H.R.M.)
[2] Department of Rangeland and Watershed Management, Faculty of Agriculture and Natural Resources, Water Management Research Center, University of Mohaghegh Ardabili, Ardabil 56199-11367, Ardabil, Iran
* Correspondence: z.hazbavi@uma.ac.ir; Tel.: +98-45-3150-5150

Abstract: In response to novel and complex uncertainties, the present research is conducted to characterize the most significant indicators of watershed health including drought, water quality, and vegetation for the Tajan watershed, Mazandaran, Iran. The Standardized Precipitation Index (SPI) and Streamflow Drought Index (SDI) are, respectively, used to quantify the meteorological and hydrological droughts in the present (1993–2020) and future (2023–2050) employing optimistic RCP2.6 and pessimistic RCP8.5 scenarios. To concoct discharge data for the future, IHACRES v1.0 software is used with a Nash–Sutcliffe coefficient (NSE) of 0.48 and a coefficient of determination (R^2) of 0.58. Maps of land use and Normalized Difference Vegetation Index (NDVI) are also prepared using Landsat images. Subsequently, the surface water quality is assessed using AqQA v1.1.0 software. The results show the difference in the severity of future meteorological droughts in different stations. In addition, the predominance of non-drought (SDI $\geq$ 0) or mild drought ($-1 \leq$ SDI < 0) is indicated for future hydrology. The land use changes show a decrease in rangeland (−5.47%) and an increase in residential land (9.17%). The water quality analysis also indicates an increase in carbonate ions in the watershed outlet. Communicating the relationships between study indicators, which is a big gap in the current watershed management approach, avoids future failures and catastrophes.

Keywords: climate fluctuations; hydrology; land cover analysis; water quality; watershed assessment; Northern Iran

Citation: Avand, M.; Moradi, H.R.; Hazbavi, Z. Interactive Changes in Climatic and Hydrological Droughts, Water Quality, and Land Use/Cover of Tajan Watershed, Northern Iran. *Water* **2024**, *16*, 1784. https://doi.org/10.3390/w16131784

Academic Editor: Didier Orange

Received: 8 May 2024
Revised: 19 June 2024
Accepted: 20 June 2024
Published: 24 June 2024

1. Introduction

The proper functioning of a watershed influences the appropriate and principled access to ecosystem services, characteristics, functions, or ecological processes that contribute to human well-being [1,2]. Assessing the watershed's ability to perform expected functions depends on overall watershed health. However, in recent decades, various natural and human-induced driving forces such as climate change, drought, flood, deforestation, population growth, overgrazing, erosion, and sedimentation have significantly impacted the health of watersheds [2,3].

Climate change and human activities, specifically changes in land use/cover, are widely recognized as the most significant factors impacting watershed health [4,5]. The destruction of natural resources and changes in land use, along with industrial growth and development, has led to an increase in greenhouse gas production [6]. Due to the rise in greenhouse gases, the climate in various regions is changing, leading to global warming. According to the Intergovernmental Panel on Climate Change (IPCC), the Earth's average surface temperature has increased by approximately 0.6 °C in the last century. It is projected that this increase will range from 1.4 to 5.7 °C by the year 2100. It is anticipated that these

changes in temperature and precipitation will have a significant impact on the planet's ecosystems [7].

Iran has not been immune to these changes. In recent years, it has experienced numerous natural hazards, such as floods, droughts, and pests, due to changes in climatic variables [8–11]. The frequency and severity of these hazards are on the rise. Climate plays a significant role in various natural hazards, including drought, which can have a profound impact on the economy and people's lives. This is particularly true in sectors such as agriculture, animal husbandry, and industry, where it can cause damage and destruction in different regions. Iran is currently facing one of its biggest climatic challenges in recent years: drought [12,13].

"A drought is a period of abnormally dry weather characterized by a prolonged deficiency of precipitation below a certain threshold over a large area and a period longer than a month" [14]. Drought is also classified according to the affected domain as meteorological, agricultural, hydrological, and socioeconomic. Each individual component, as well as the overall total, has an impact on various aspects of the watershed. For instance, climatic changes have a significant impact on the temporal and spatial distribution of precipitation in various regions, leading to numerous problems. One of the most significant differences between drought and other natural disasters is its gradual process and slow speed. It may take several years or even longer for the effects to become evident, making it different from other hazards [15]. It is a sluggish, risky phenomenon, so the mental impacts on living organisms from drought are more delicate and prolonged than other disasters [16]. However, the applicability of different time scales in the assessment of drought conditions is important since each can capture something different, which is highly relevant to, for example, agriculture or hydrology. Recent research has highlighted that droughts are increasing over shorter time scales, but their overall duration is shortening, indicating that there is a sustained short-term climatological trend in drought [17,18]. Longer time scales for drought identification show a reduced occurrence of drought, but each occurrence is prolonged [17,18].

Land use change, as another dynamic component of an ecosystem, has been affected by human activities, and along with the phenomenon of climate change, it has increased the severity of risks and environmental disturbances [19–23]. As a result of the increase in population in the past years and the increase in demand for resources, food, and energy, a large area of wilderness forest and rangelands was subjected to excessive pressure and destruction, and the result of these changes is clearly visible in the occurrence of today's dangers [23–26]. The most important effects of land use change that are currently occurring as human threats and reducing the health of the ecosystem are the phenomena of dust, increase in runoff and flooding, decrease in oxygen and increase in CO_2, decrease in biodiversity, etc. [24]. Furthermore, the impact of climate change and land use/cover causes changes in other watershed components such as runoff and water quality [5,24,27–33]. The land use and vegetation in an area can directly impact the water quality and overall health of the watershed [34–39]. Therefore, as it is known, the various components in a watershed are related to each other in a complex way, and changes in each of these components cause changes in other components.

The literature also depicts the interactive impact of watershed health indicators in different conditions. For example, Mishra et al. [25] studied the potential effects of extreme weather-related disasters (e.g., drought, floods, and wildfires) on various water quality in the Carolinas, the United States of America. The results showed that flooding leads to high levels of pollution-related bacteria, especially in the river environment. The impact of drought on water quality indicators in different land use environments can be different, which highlights the dominant role of watershed characteristics. In addition, in Thailand, Khadka et al. [40] predicted the effects of climate and land use changes on future droughts (2021–2050) in one of the main branches of the Mekong River. Both climate and land use changes had significant effects on drought-sensitive agriculture. In addition, in the Metropolitan region of Chile, drought indices were used to describe meteorological and

hydrological droughts for the period 1985 to 2015. To understand the relationship between drought and water quality, the correlation between daily discharge and surface water quality observations was evaluated. A significant negative relationship ($p < 0.05$) was observed between discharge and electrical conductivity and major ions in most of the region. Hydrological stations located in irrigation areas exceed the allowed threshold [41].

Assessing the ecosystem conditions affected by natural and human-induced hazards, such as drought and land use changes, is particularly important at the watershed level and over different time periods to facilitate effective decision-making and management. The Tajan watershed, a crucial ecosystem in Mazandaran province, faces destruction and decline due to various factors [42]. These factors include severe land use changes driven by increasing land prices, deforestation, reduced water resources caused by climate change, increased damages from floods and droughts, changes in surface water quality due to land use changes, and the use of agricultural pesticides and industrial effluents [43]. Therefore, the study of interactive changes in the most impact-causing driving forces of watershed health degradation in this watershed is highly crucial, but these driving forces have not been considered yet. This research also tries to fill the gaps related to the prediction of climatic and hydrological drought simultaneously in different scenarios and its relationship with land use and the greenness index. Our findings suggest various scenarios to address and adapt to these changes to mitigate destruction, and the promotion of watershed sustainability could be proposed.

2. Materials and Methods

2.1. Study Area

This research was conducted in the Tajan watershed (53°18′ to 53°05′ E longitude and 36°29′ to 36°09′ N latitude), which covers an area of 3980 Km^2 (Figure 1). This watershed, located upstream of Sari and Neka cities in Mazandaran province, is one of the largest watersheds in Northern Iran. It is bordered by the Alborz Mountains to the south and the Caspian Sea to the north. The watershed is extensive, spanning across six cities: Neka, Ghaemshahr, Sari, Behshahr, Damghan, and Savadkuh. The average annual temperature of the watershed is approximately 15 °C, having a hot and humid climate. The region receives an average rainfall of 832 mm annually [42]. The altitude ranges from −2 m to 3718 m asl, with the outlet closed above the Caspian Sea inlet. The majority of the studied area consists of forest lands, with agricultural lands limited to river banks or sloping areas in certain regions.

The primary occupation of local communities, particularly in the upstream villages, is predominantly agriculture and animal husbandry. Due to favorable weather conditions, the tourism industry has been somewhat active in recent years, leading to changes in land use in various areas of this watershed. In addition to the well-known Tajan river, this area is also home to other major branches such as Chahardange, Dodange, Lajim, and Zarmrud. These rivers flow through different villages before eventually reaching the Caspian Sea. This watershed is selected for the present study because it contains numerous ecosystems and important water sources and rivers that provide drinking water and support agriculture for local and urban communities downstream.

2.2. Methodology

2.2.1. Data Sources and Processing

The essential climatic data (1993–2020) needed for climate modeling, forecasting, and meteorological drought investigation, including precipitation, maximum and minimum temperature, and sunshine hours or radiation, are collected from the Mazandaran Meteorology General Office (https://www.mazmet.ir/en/, accessed on 5 April 2022). To predict future climate patterns, climate data are collected from three synoptic and rain gauge stations (i.e., Kordkhil, Soleyman tangeh, and Rig Cheshmeh), located in or near the study area (Figure 1). These stations were selected based on their suitable distribution and consistent time period.

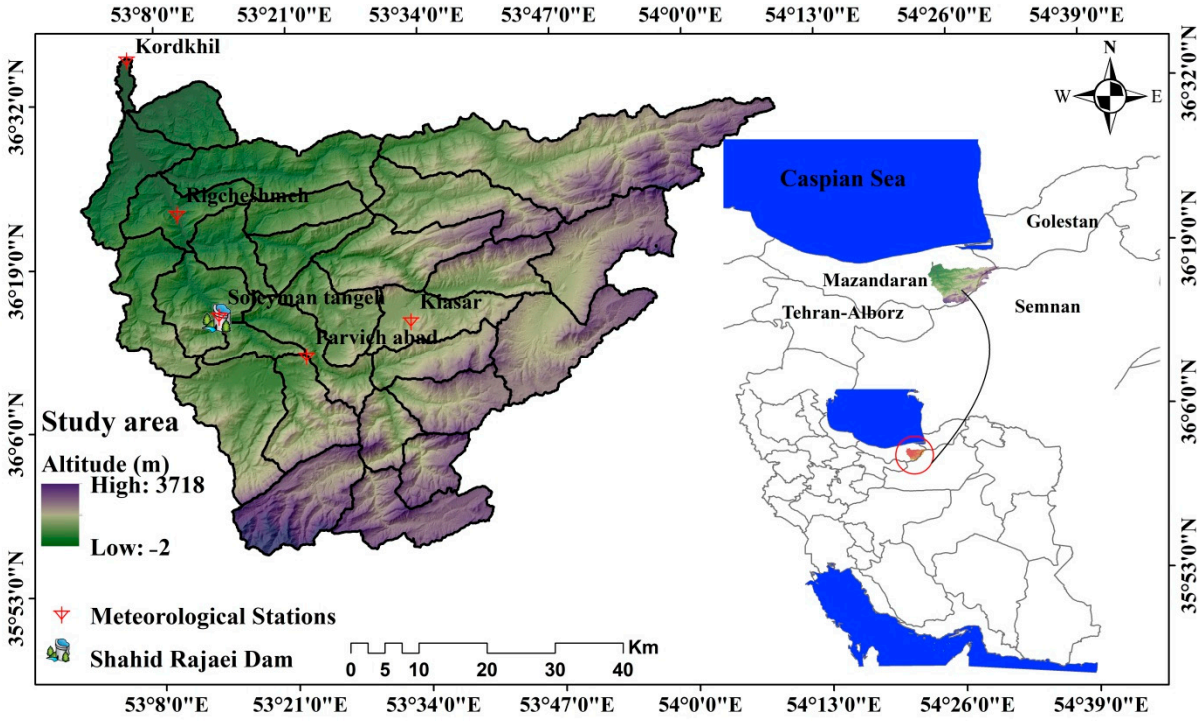

Figure 1. Geographical location of Tajan watershed in Mazandaran province, Iran.

Lars-WG v6.0 software is utilized to forecast future climate conditions (2023–2050) based on two climate scenarios: optimistic (RCP2.6) and pessimistic (RCP8.5) [44]. DrinC v1.7 software is also used to determine drought thresholds based on the SPI standard table, using current and future data.

Additionally, existing hydrometric stations in the region with more complete data are used to investigate the trend of flow discharge changes. The data from the hydrometric stations are obtained from the Mazandaran Regional Water Authority (https://www.mzrw.ir/?l=EN, accessed on 5 April 2022). The time series of the hydrological data spans from 1997 to 2017 for the base period and from 2021 to 2040 for the future period. The IHACRES hydrological model was utilized to forecast future discharge. The trend of future discharge data is predicted using long-term data on precipitation and temperature, along with observed discharge. The hydrological drought at the outlet station (Kordkhil) is then calculated using the SDI in DrinC v1.7 software [15]. After analyzing the stream flow data and using the standard table for the SDI, the thresholds for hydrological drought were determined.

AqQA v1.1.0 software was used to analyze the trends and characteristics of surface water quality at two stations of Kordkhil and Parvich abad (Figure 1), over 20 years. Finally, the trend of land use/cover changes and their impact on parameters such as water quality and runoff were analyzed using Landsat satellite images.

2.2.2. Climatic Drought Calculation

The Standardized Precipitation Index (SPI) is a powerful tool for analyzing rainfall data [45]. This index assigns a numerical value to rainfall, allowing for comparisons between areas with different climates. It also establishes a quantitative index for assessing current drought conditions. The SPI quantifies the lack of precipitation across various time scales. The main feature of this index is its flexibility in measuring droughts across various time scales, as droughts can vary greatly in terms of duration. It is important to detect and monitor these risks using various time scales. The SPI for each region is calculated using long-term rainfall statistics for various time periods. The long-term statistic is fitted to the gamma probability function, which is then used to calculate the cumulative probability of

rainfall for a specific station, month, and time scale. When calculating the SPI, the first step is to select a suitable probability distribution function that can accurately represent a long series of observed rainfall data. The Gamma distribution has been widely used in various studies as an effective model for describing rainfall data. The cumulative probability of the observed rainfall data is calculated. The cumulative probability is transformed using the inverse normal Gaussian function with a mean of 0 and a variance of 1 to calculate the SPI for 3, 6, and 12 months [8,12]. The gamma distribution is defined by the probability density function (Equation (1)).

$$f(x, a, \beta) = \frac{1}{\beta^a \Gamma(a)} x^{a-1} e^{-x/\beta}, \; for \; x, \; a, \; \beta > 0 \tag{1}$$

where a is the shape and β shows the scale parameters, and these scale parameters can be obtained by maximum likelihood estimation. The standard classification of this index is presented in Table 1.

Table 1. Climatic drought classification based on SPI [45,46].

Row	Classification	SPI Value
1	Super humid	≤ 2
2	Very humid	1.99 to 1.5
3	Relatively humid	1.49 to 1
4	Near normal	0.99 to −0.99
5	Moderate drought	−1 to −1.49
6	Severe drought	−1.5 to −1.99
7	Extreme drought	≤ -2

2.2.3. Hydrological Drought Calculation

The Streamflow Drought Index (SDI) is used to investigate hydrological drought. This index is similar to the SPI in terms of calculations, but it is recommended for use on a monthly and seasonal time scale. The SDI, developed by Nalbantis [47], is based on the standard monthly flow (Equation (2)).

$$SDI_{ik} = \frac{V_{ik} - V_k}{S_k} \; i = 1, 2, \ldots \; k = 1, 2, 3, 4 \tag{2}$$

This equation assumes that in the time series of monthly river flows, i represents the hydrological year and k represents the corresponding month. V_k and S_k represent the average and standard deviation, respectively, of the total flow volume for the base period k. V_{ik} refers to the cumulative volume of river flow during the base period. The standard classification of SDI is presented in Table 2.

Table 2. Hydrological drought classification based on SDI [47,48].

Condition	Classification	SDI Value
0	Non-drought	$SDI \geq 0$
1	Mild drought	$0 \leq SDI < -1$
2	Moderate drought	$-1 \leq SDI < -1.5$
3	Severe drought	$-1.5 \leq SDI < -2$
4	Extreme drought	$SDI < -2$

2.2.4. IHACRES Hydrological Model

IHACRES is a conceptual rainfall–runoff model that was initially developed by Jakeman et al. [49]. The model has been successfully applied to watersheds with various sizes, ranging from 490 m^2 in China to 10,000 Km^2 in England, and with time intervals ranging from 6 min to 1 month. To implement this model, data inputs such as precipitation, temper-

ature, and flow discharge are required. Temperature and precipitation are used to simulate flow discharge, which is then used to calibrate and evaluate the accuracy of the model [50].

IHACRES comprises two nonlinear reduction modules and a linear hydrograph module. To implement this model, rainfall and temperature are first converted to effective rainfall in each time step using the nonlinear module. Then, the single hydrograph's linear module converts it to surface runoff within the same time step [51]. This model consists of six parameters. Three parameters, c (moisture storage capacity of the watershed), tw (the time it takes for the watershed to dry), and f (watershed temperature adjustment factor), are related to the nonlinear loss component of the model. The other three parameters, tq, ts (the time it takes for fast and slow flow to decrease, respectively), and Vs (the volume of slow flow that contributes to river flow), are related to the linear function component of the model [52]. In this research, the default value of key parameters of the model was used. The discharge in the selected hydrometric station is predicted using the IHACRES model. This prediction is based on climate forecasts, including precipitation and temperature data, as well as the current discharge.

For the simulation, the data of daily precipitation, average daily temperature, and daily discharge of the statistical period (1997–2017) of Kordkhil station were entered into IHACRES v1.0 software, and a time period of 2 years (730 days) was determined for model warm-up. In addition, the period of 1997–2008 was chosen as the calibration period, and the period of 2009–2017 was chosen as the validation period.

To simulate the daily discharge in the Tajan watershed from 2021 to 2040, we used precipitation, temperature, and discharge data from the Kordkhil station. This station was chosen as the main and outlet station for the watershed due to its suitable data. The data needed to run the rainfall–runoff model and predict future discharge includes future precipitation, future temperature, and the base discharge of the desired station. The precipitation and temperature are modeled in previous stages for the future time. The model was calibrated for the period 1997–2012. The period was determined through a trial-and-error process, and the period with the most successful simulation was ultimately chosen. The model was evaluated in the remaining period. The IHACRES model execution diagram is shown in Figure 2.

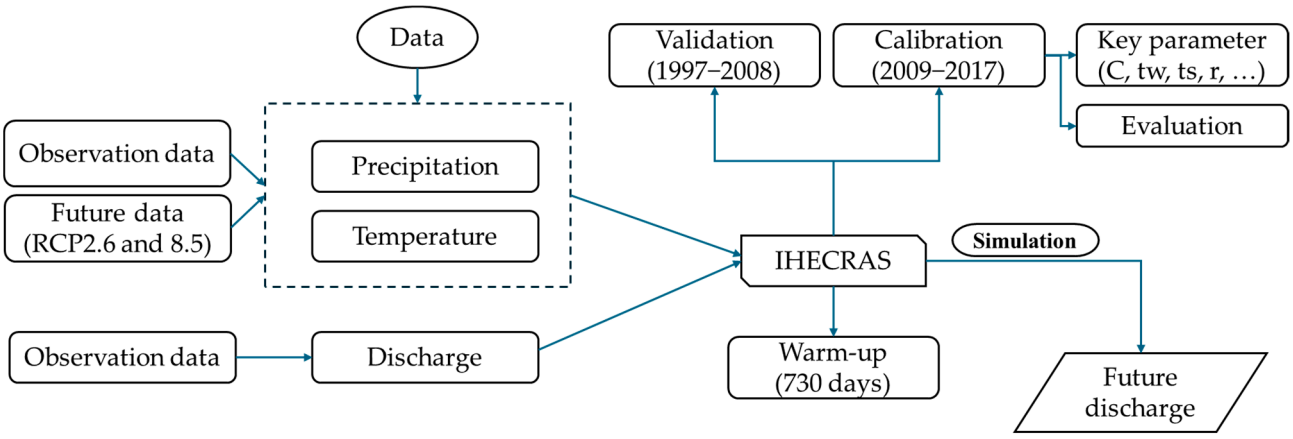

Figure 2. Diagram of the implementation of the hydrological model of IHACRES.

2.2.5. Surface Water Quality Assessment

The surface water quality is examined by analyzing data from two hydrometric stations: Kordkhil station (downstream) and Parvich abad station (upstream) (Figure 1). We used a suitable time period (2001–2021) to investigate the trend of quality changes. The data analyzed in this research to determine water quality include electrical conductivity (EC), total dissolved solids (TDS), chloride (Cl^-), sodium (Na^+), potassium (K^+), sodium absorption ratio (SAR), and bicarbonate. The substances measured in this study include bicarbonate (HCO_3), calcium (Ca^{2+}), magnesium (Mg^{2+}), sulfate (SO4), and acidity (pH^+).

To assess the surface runoff potential for drinking water and agriculture, various charts such as Schuler (for drinking water) and Wilcox (for agricultural water) are utilized in AqQA v1.1.0 software. Moreover, to check the trend of ions in the past years, the Mann–Kendall test [53,54] and ordinary-least-square (OLS) regression slope [55] are used.

2.2.6. Trend Analysis and Predicting Land Use/Cover Change

Available sensors and satellite images were utilized for this study, ensuring compatibility with other data. Land use data are prepared using Landsat satellite images based on the TM, ETM+, and OLI sensors for three span times: 1991, 2010, and 2020. First, pre-processing was conducted on satellite images, and field surveys were conducted in June and July 2019 to obtain training samples. The land use classes in the study area are monitored using the maximum likelihood algorithm, which is a conventional method known for its high accuracy [24,29,56].

To investigate the impact of drought on vegetation in the studied watershed, the Normalized Difference Vegetation Index (NDVI) time series [57] from Landsat satellite images was analyzed [58] over a 20-year period (2001–2020). The LCM method was utilized in TerrSet 19.0.8 software to forecast future land use conditions. To achieve this, this study initially examined land use changes over the study period. Subsequently, various scenarios were evaluated to determine the most accurate implementation sub-model and independent variables. These variables, including the Digital Elevation Model (DEM), slope, distance from residential areas, waterways, roads, and agricultural lands, are found to have a strong correlation with land use changes in the study area. The transformation of each land use and the prediction of land use changes are also modeled using a multi-layer perceptron function and Markov chain. Kappa coefficients and overall accuracy were used to assess the accuracy of the land use maps that are created. TerrSet 19.0.8 software and ENVI 5.5.2 software [56] were utilized for all the mentioned steps.

3. Results and Discussion

3.1. Results of Climatic Drought Assessment

Figure 3 displays the trend of climatic drought based on observational data from various stations between 1993 and 2020. Changes in meteorological drought conditions over a 27-year period indicate climate fluctuations, which are signs of climate change in the region. Based on the obtained results, it cannot be definitively stated that the next 30 years will be consistently dry or wet, although it is necessary to use adaptation approaches to mitigate the long-term effects of drought.

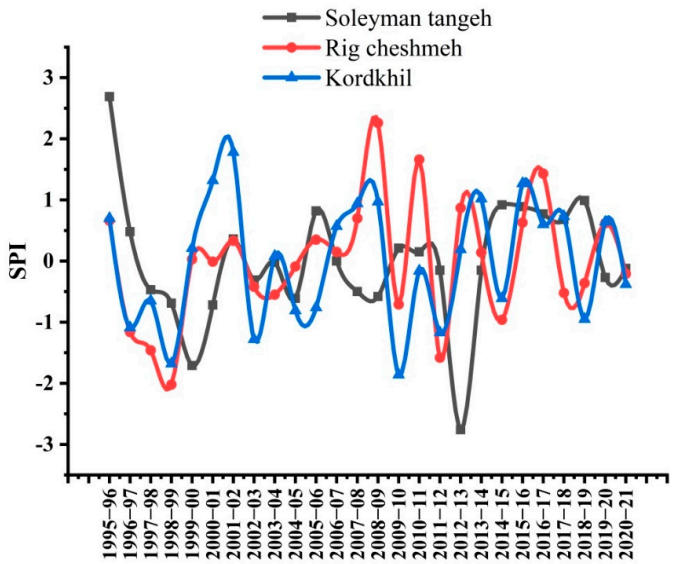

Figure 3. Climatic drought trends in the basic observational data of different stations.

The findings indicate that the level of drought has varied between −3.3 (indicating very severe drought) and 2.4 (indicating extremely humid conditions) in recent years. Moreover, in Figure 4 and Table 3, the forecast of the future drought condition for a period of 27 years (2023–2050) under the influence of two optimistic (RCP2.6) and pessimistic (RCP8.5) scenarios is shown.

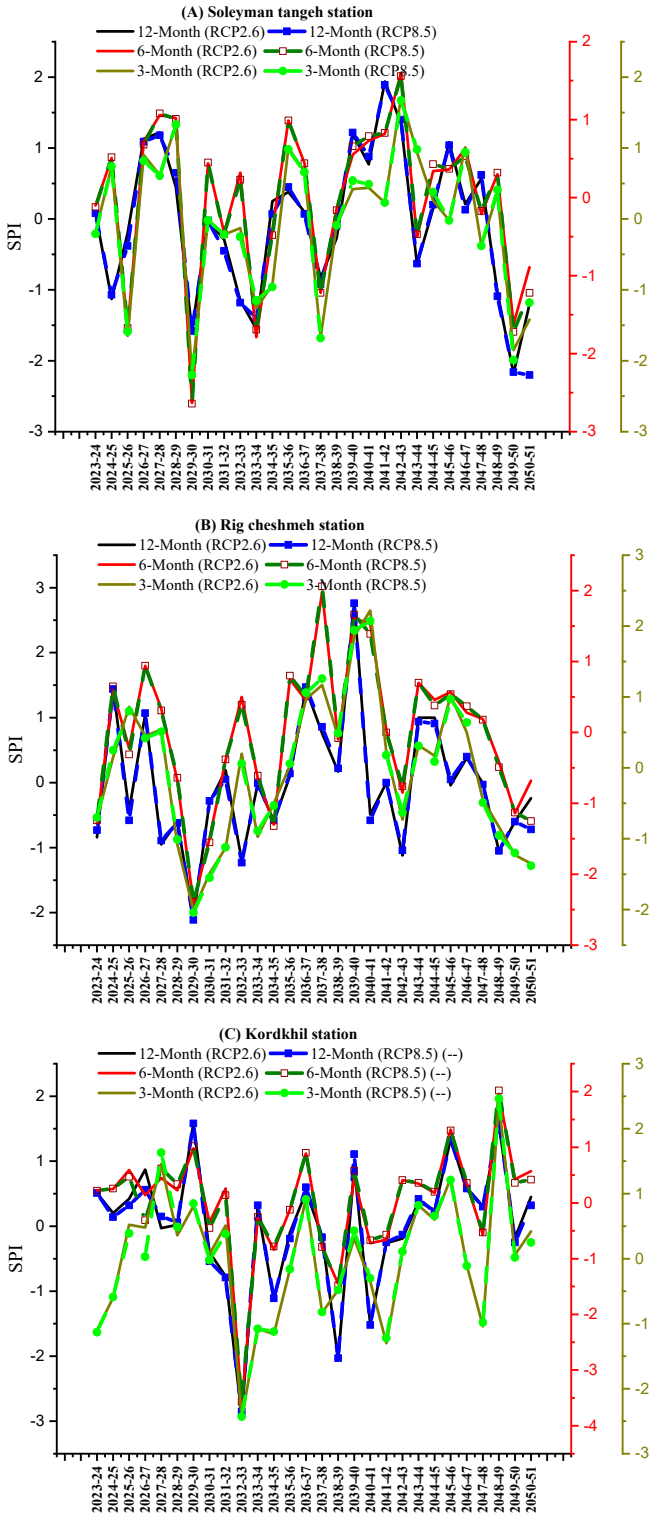

Figure 4. The change trend of SPI in different time steps and different scenarios of (**A**) Soleyman tangeh, (**B**) Rig Cheshmeh, and (**C**) Kordkhil stations.

Table 3. Meteorological drought situation of Tajan watershed stations in the future using two climate scenarios.

Station	Soleyman Tangeh				Rig Cheshmeh				Kordkhil			
Year	SPI (RCP2.6)	Class *	SPI (RCP8.5)	Class *	SPI (RCP8.5)	Class *	SPI (RCP8.5)	Class *	SPI (RCP8.5)	Class *	SPI (RCP8.5)	Class *
2023–24	0.08	4	0.08	4	−0.84	4	−0.73	4	0.51	4	0.51	4
2024–25	−1.13	5	−1.07	5	1.45	3	1.44	3	0.2	4	0.14	4
2025–26	−0.2	4	−0.38	4	−0.43	4	−0.58	4	0.42	4	0.32	4
2026–27	1.13	3	1.09	3	1.05	3	1.07	3	0.87	4	0.56	4
2027–28	1.22	3	1.18	3	−0.95	4	−0.89	4	−0.03	4	0.15	4
2028–29	0.45	4	0.65	4	−0.6	4	−0.62	4	0.02	4	0.06	4
2029–30	−1.57	6	−1.58	6	−2.07	7	−2.11	7	1.59	2	1.58	2
2030–31	−0.03	4	−0.02	4	−0.31	4	−0.28	4	−0.4	4	−0.54	4
2031–32	−0.29	4	−0.45	4	0.19	4	0.05	4	−0.77	4	−0.79	4
2032–33	−1.15	5	−1.18	5	−1.2	5	−1.23	5	−2.92	7	−2.85	7
2033–34	−1.55	6	−1.4	5	−0.02	4	−0.01	4	0.28	4	0.32	4
2034–35	0.25	4	0.07	4	−0.59	4	−0.58	4	−1.14	5	−1.11	5
2035–36	0.38	4	0.45	4	0.1	4	0.14	4	−0.1	4	−0.19	4
2036–37	0.1	4	0.07	4	1.44	3	1.47	3	0.53	4	0.6	4
2037–38	−0.83	4	−0.92	4	0.76	4	0.86	4	−0.15	4	−0.17	4
2038–39	−0.27	4	−0.1	4	0.17	4	0.22	4	−2.05	7	−2.03	7
2039–40	1.2	3	1.22	3	2.77	1	2.76	1	0.9	4	1.11	3
2040–41	0.77	4	0.88	4	−0.49	4	−0.58	4	−1.51	6	−1.52	6
2041–42	1.94	2	1.89	2	0	4	0	4	−0.26	4	−0.25	4
2042–43	1.35	3	1.4	3	−1.12	5	−1.04	5	−0.19	4	−0.13	4
2043–44	−0.64	4	−0.63	4	1	3	0.94	4	0.38	4	0.42	4
2044–45	0.15	4	0.2	4	1	3	0.91	4	0.25	4	0.22	4
2045–46	1.08	3	1.04	3	−0.04	4	0.05	4	1.34	3	1.33	3
2046–47	0.21	4	0.13	4	0.38	4	0.4	4	0.56	4	0.58	4
2047–48	0.57	4	0.62	4	−0.01	4	−0.03	4	0.31	4	0.3	4
2048–49	−1.03	5	−1.09	5	−1.05	5	−1.05	5	1.57	3	1.65	2
2049–50	−2.18	7	−2.16	7	−0.6	4	−0.6	4	−0.18	4	−0.25	4
2050–51	−1.2	5	−2.2	5	−0.24	4	−0.72	4	0.45	4	0.32	4

Notes: * Super humid (1). Very humid (2). Relatively humid (3). Near normal (4). Moderate drought (5). Severe drought (6). Extreme drought (7).

The SPI for Rig Cheshmeh station in the pessimistic scenario range from 2.76 to −2.11. Its lowest value is expected to occur in 2029–2030 during a very severe drought, while the highest value is expected in 2039–2040 (extremely humid). In addition, the index values for the Rig Cheshmeh station in the optimistic scenario vary from 2.77 to −2.07. Its lowest value will occur in 2029–2030 (very severe drought) and the highest value will occur in 2039–2040 (extremely humid). Therefore, it can be expected that, in the water year 2029–2030, there is a possibility of a very severe drought in this region. As a result, it is crucial to take the necessary measures to address this potential climatic challenge.

The SPI values for Soleyman tangeh station in the pessimistic scenario range from 1.89 to −2.16. The lowest value (−2.16) was obtained in 2049–2050 during a very severe drought, while the highest value (1.89) was obtained in 2041–2042 during very wet conditions. In addition, the values of this index for Soleyman tangeh station in the optimistic scenario vary from 1.94 to −2.18. The lowest value occurs in 2049–2050, indicating a very severe drought, while the highest value is observed in 2041–2042, indicating relatively

wet conditions. Therefore, it can be expected that in the water year 2049–2050, there is a possibility of a severe climatic drought in this region. In addition, the results show no significant difference in the future drought index between the two scenarios.

The SPI values for Kordkhil station in the pessimistic scenario vary from 1.58 to −2.85. The lowest value (−2.85) is expected in 2032–2033, indicating a very severe drought. On the other hand, the highest value (1.58) is projected in 2029–2030, indicating a very humid condition. In the optimistic scenario, the Kordkhil station will experience its lowest value of this index in 2032–2033 (−2.92, indicating a very severe drought) and its highest value in 2029–2030 (1.59, indicating a very wet period). Therefore, the results of Kordkhil station are somewhat different compared to the other two stations that are located at a higher altitude, and this difference is probably due to the proximity of this station to the Caspian Sea and the climate of that region being affected by the humidity of the coast. It can also be expected that there will be a very severe climatic drought in the water year 2032–2033. Therefore, the results of this research regarding the increase in drought periods compared to the base period are in accordance with the findings of [43].

3.2. Results of Hydrological Drought Assessment

Figure 5 illustrates the drought trend based on observation data from two hydrometric stations using the SDI. The data span a 30-year period (1990–2021) and is analyzed in 12-month increments. In this study, two hydrometric stations were used to accurately measure the amount of discharge in both the upstream and downstream areas of the watershed. Therefore, the Parvich abad station (upstream), the Kordkhil station (downstream), and the outlet of the watershed are selected.

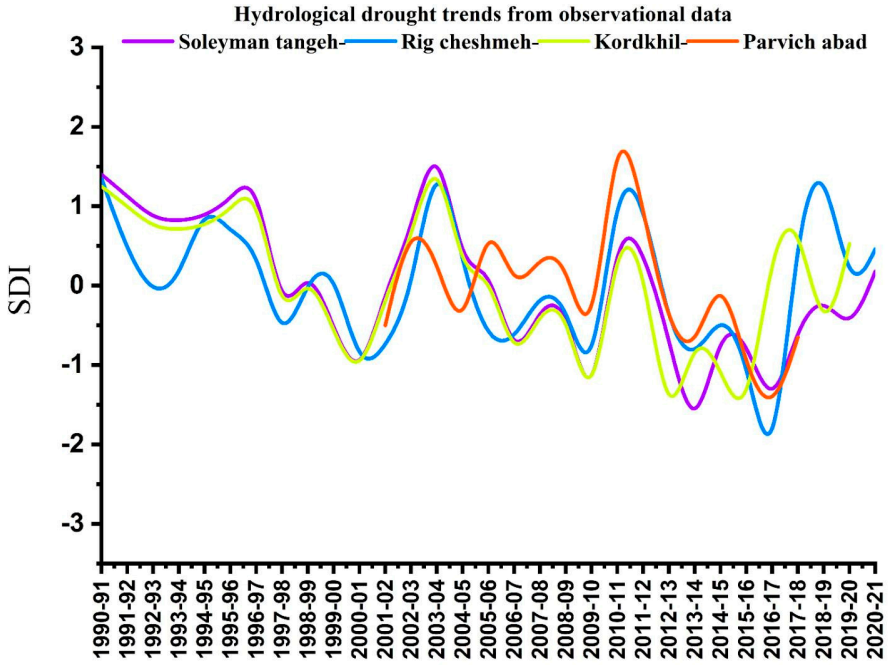

Figure 5. Hydrological drought trend of observational data of selected stations.

Figure 6 shows the comparison graph of the simulated and observed discharge of Kordkhil station. The IHACRES model accurately simulates the discharge, and the two graphs show a high level of agreement, as depicted in Figure 6.

Table 4 shows the results of the rainfall–runoff model simulation. Herein, both values are measured in mm y^{-1}. The coefficient values obtained in the two stages of evaluation and recalibration were 0.48 and 0.53, respectively, which are consistent with the findings of Tramblay et al. [59]. This model is very sensitive to the time matching of rainfall and discharge, and due to the lack of comprehensive data in the study area, it was not possible to

implement it for different stations with similar time periods. In addition, the data obtained from the prediction of the Lares-WG climate model as well as the observational data of discharge have uncertainty, which has caused a slight deviation in the model results.

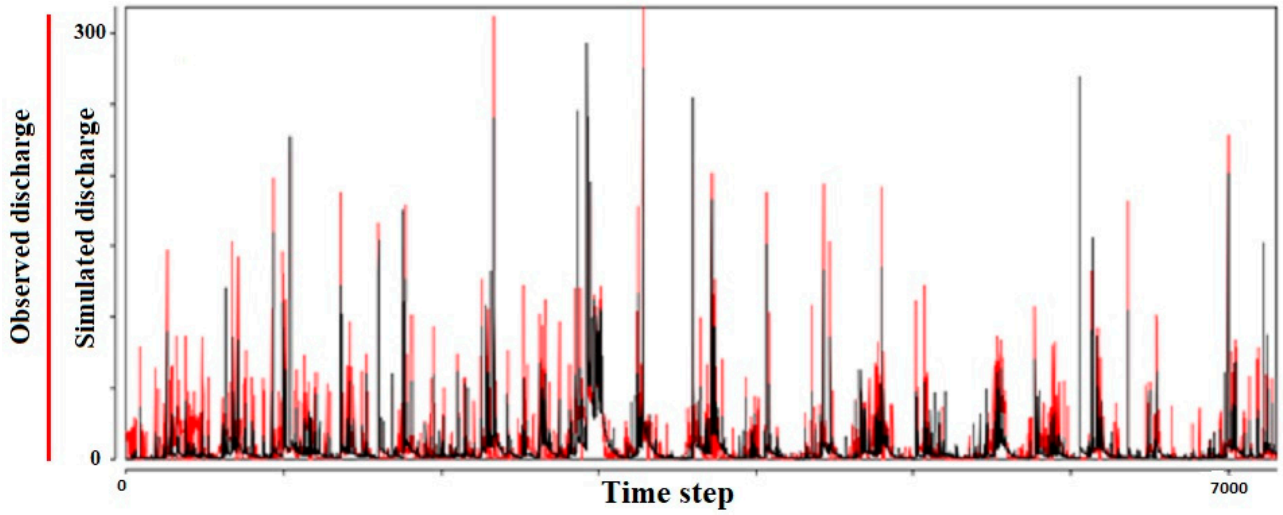

Figure 6. Comparison of simulated discharge (2021–2040) and observations (1997–2017) in the calibration phase of the hydrological model.

Table 4. The results of calibration and evaluation of the model at the Kordkhil station of the Tajan watershed in the period of 1997–2017.

Station	Stage	Time Step	R Squared	Nash–Sutcliffe Coefficient (NSE)	Bias (mm y^{-1})	Q (mm y^{-1}) *	P (mm y^{-1}) *
Kordkhil	Calibration	Daily	0.64	0.53	21.12	48.7	673.13
	Validation	Daily	0.58	0.48	26.16	61.22	838.23

Notes: * Q represents the portion of precipitation that contributed to the formation of the watershed river throughout the measurement and evaluation period, while P represents the total precipitation during that period.

Figure 7 shows the results of analyzing the hydrological drought trend at the Kordkhil station. The analysis was conducted using the SDI over a 20-year period, with time intervals of 3, 6, and 12 months. The analysis considered both the RCP8.5 and RCP2.6 scenarios. The figures clearly indicate that the most significant drought changes in the future period, in both scenarios, will occur every three months. The magnitude of these changes will range from −1.5 (moderate drought) to 3.5 (non-drought). The results indicate that climate change has not had a significant impact on discharge. The likely cause of this is heavy rainfall events resulting from climate change, which leads to an increase in flash floods in the river. The research findings only show the effect of climate change on discharge, and it is possible that other factors like changes in land use may also have an influence. The results of this research are somewhat consistent with the findings of previous research [4] regarding the limited impact of climate change on runoff. Xue et al. [4] discovered that human activities, such as alterations in land use, have had a greater influence on runoff than climate change. Zhang et al. [33] also demonstrated the significant influence of climate change on runoff in comparison to land use. The results of the present study also indicate that the discharge of the Tajan watershed is unlikely to change significantly in the future due to climate change. However, there is a possibility that other factors such as land use change or water transfer may decrease the discharge of the Tajan river.

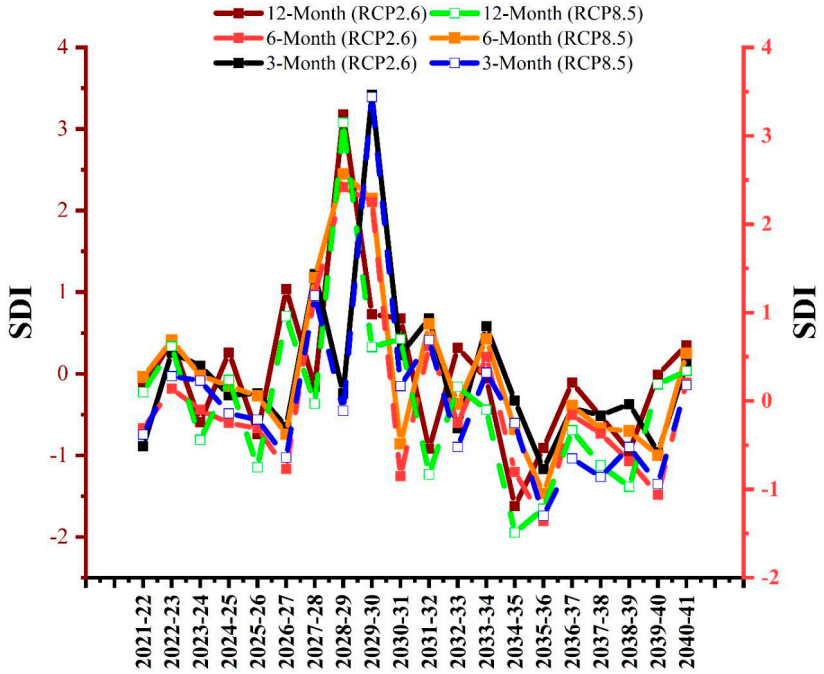

Figure 7. Future hydrological drought trend of Kordkhil station using two optimistic (RCP2.6) and pessimistic (RCP8.5) scenarios.

The hydrological drought situation and index values for the predicted period (2021–2040) of Kordkhil station are presented in Table 5. The analysis was conducted using a time step of 12 months and two scenarios, RCP2.6 and RCP8.5, with the SDI. The values of this index for Kordkhil station in the pessimistic scenario range from 3.15 to −1.49. The lowest value, indicating a moderate drought, is expected to occur in 2034–2035 (−1.49), while the highest value, indicating no drought, is projected for 2028–2029 (3.15). The index values for Kordkhil station in the optimistic scenario range from 3.18 to −1.62. The lowest value, indicating severe drought, is projected to occur in 2034–2035 (−1.62), while the highest value, indicating no drought, is expected in 2028–2029 (3.18). Since this station is situated at the outlet of the watershed and receives most of the runoff from the upstream watershed, the river's discharge is typically high and less influenced by changes. Additionally, the region's proximity to the Caspian Sea has led to increased rainfall, resulting in higher runoff. These findings are consistent with the research conducted by Kazemzadeh and Malekian [19]. Based on the available results, there is a high likelihood of severe hydrological drought in both scenarios in 2034–2035. This drought is likely caused by changes in precipitation during this period. Therefore, it is crucial to take necessary measures in the year before, during, and after to minimize the impact on water farmers along the Tajan river. Prior notifications should be given to encourage appropriate farming practices during those years.

The investigation of the hydrological drought index (SDI) compared to the meteorological drought index (SPI) in the future indicates their compatibility in most years. There is a notable increase in precipitation from 2028 to 2030 (Figure 8). There is also the possibility of a wet year between 2039 and 2041. The most severe drought is projected to occur between 2034 and 2036. Therefore, in the future, we can expect alternating periods of drought and wet years. It is important to take measures to adapt and mitigate the associated risks. The climate fluctuations result in heavy rainfall, floods, and increased stream flow during certain times of the year. The amount of flow in an area is not solely determined by precipitation; factors such as land use and cover also significantly influence runoff [15,48].

Table 5. Hydrological drought condition of Kordkhil station in the future under two different scenarios.

Station	Kordkhil			
Year	SDI (RCP8.5)	* Class	SDI (RCP8.5)	* Class
2021–22	−0.17	1	0.1	0
2022–23	0.4	0	0.62	0
2023–24	−0.59	1	−0.44	1
2024–25	0.26	0	0.24	0
2025–26	−0.74	1	−0.75	1
2026–27	1.04	0	0.96	0
2027–28	−0.16	1	−0.03	1
2028–29	3.18	0	3.15	0
2029–30	0.73	0	0.61	0
2030–31	0.68	0	0.7	0
2031–32	−0.92	1	−0.83	1
2032–33	0.32	0	0.16	0
2033–34	−0.06	1	−0.1	1
2034–35	−1.62	3	−1.49	2
2035–36	−0.91	1	−1.22	2
2036–37	−0.11	1	−0.33	1
2037–38	−0.52	1	−0.73	1
2038–39	−0.95	1	−0.97	1
2039–40	−0.01	1	0.19	0
2040–41	0.35	0	0.34	0

Notes: * Non-drought (0), Mild drought (1), Moderate drought (2), Severe drought (3), Extreme drought (4).

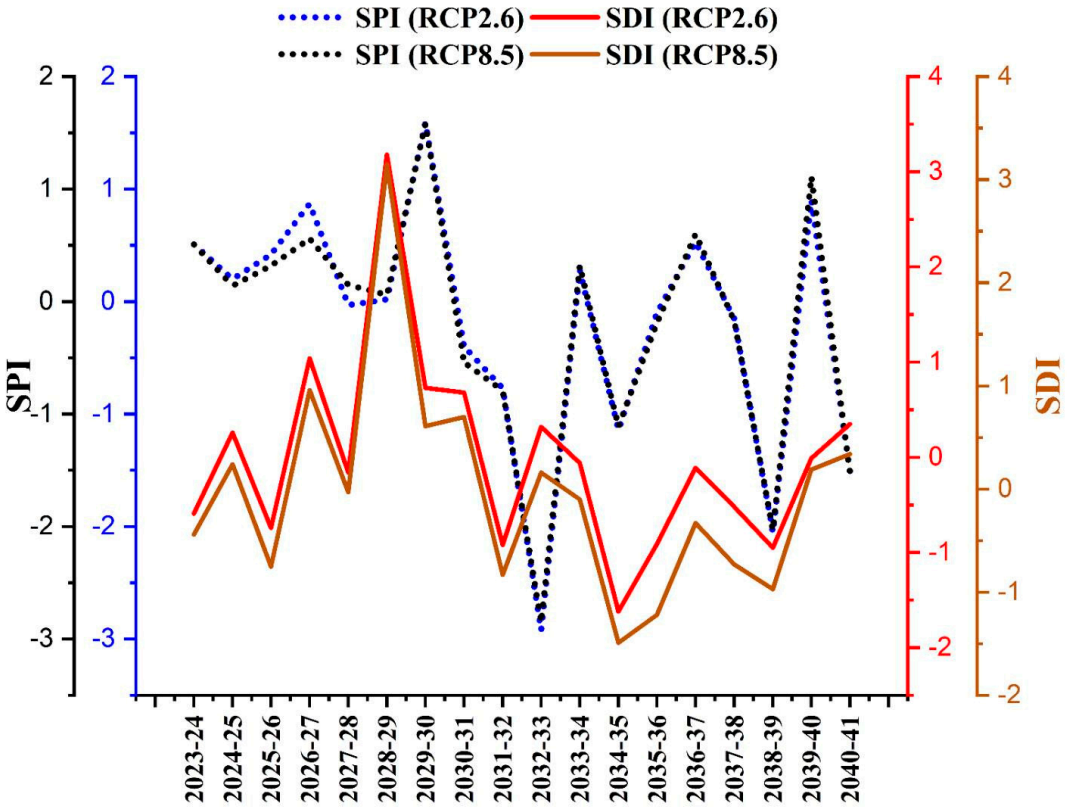

Figure 8. The trend of future changes in SPI relative to SDI in a 12-month time step based on two scenarios RCP2.6 and RCP8.5.

3.3. Results of Surface Water Quality Assessment

The results of changes in surface water quality in the Tajan watershed at two stations, Parvich abad (upstream) and Kordkhil (downstream), is reported in Table 6. The physical

characteristics of both stations indicated the presence of calcium carbonate in the water, suggesting the existence of limestone formations in the upstream areas. The water has a high hardness due to the presence of calcium carbonate, with a concentration of 273 mg L^{-1} at the outlet.

Table 6. Physical characteristics of water quality in two studied stations.

Characteristic \ Station	Kordkhil (Downstream)	Parvich Abad (Upstream)
Type of water	Ca-HCO_3	Ca-HCO_3
Hardness (mg L^{-1})	273.75	240
Electrical conductivity (µmoh cm^{-1})	770	561
Salinity risk	High	Moderate
SAR	0.196	0.069
ESR	0.231	0.092
Magnesium risk	49.8	46.2
Dissolved solids (mg kg^{-1})	506	351
Density (g cm^3)	0.997	0.997
The difference percentage of anion and cation	53.36	52.67
Measured TDS to EC ratio	0.657	0.635

The water salinity is higher at the outlet station of the watershed. The electrical conductivity at the Kordkhil station is about 770 µmohs cm^{-1}, indicating a high risk of salinity. The changes in the sodium absorption ratio (SAR) at both stations indicate an increase in water salinization at the outlet station (Kordkhil). This raises concerns about potential soil degradation if the downstream lands are irrigated with this water. Land use/cover changes have the great impact on surface water quality. The expansion of agricultural lands resulting from the use of chemical fertilizers, along with soil erosion caused by agriculture can have an impact on water quality (Moradzadeh et al., 2024). The results also indicate an increase in the dissolution of solids at the downstream station. The changes indicate a decline in water quality at the downstream station, likely due to the convergence of multiple rivers at that location.

The conventional Wilcox diagram was used to assess the water quality for agricultural purposes. The water quality at Kordkhil station (left) is divided into two ranges, C2S1 and C3S1 (Figure 9). Given the low sodium content indicated by S1, this water is suitable for all types of soil and poses a low risk of soil degradation. C2 also indicates water with moderate salinity, which can be suitable for agricultural irrigation with proper leaching. C3 indicates that the water has high salinity, making it unsuitable for irrigating agricultural lands, particularly those with inadequate drainage. This poses a risk of land salinization.

The water quality results from the Parvich abad (right) station indicate that it is slightly better than the Kordkhil station. Therefore, the water quality at this station falls within the C2S1 class range. Therefore, this water can be safely used for agricultural irrigation. The higher quality of this station is attributed to its higher altitude and lower solute dissolution in the water.

The drinking water quality assessment of the Tajan watershed in two stations, Kordkhil and Parvich abad, is depicted in Figure 10 and Table 7. The results illustrate significant fluctuations in water quality at the Kordkhil station over the years, with the most notable decline occurring in recent years (2017–2021). This indicates a high concentration of ions in the water of the area under study. The concentration range of ions varies between 0.007 and 0.25 meq kg^{-1}. The concentration range of ions in Parvich abad station (0.003–0.15 meq kg^{-1}) is lower than that of Kordkhil station. Additionally, there is no specific trend in the water quality changes at this station. A decline in water quality can be observed in 2017–2018.

Table 7. Statistical characteristics of different chemical components of Kordkhil (1) and Parvich abad (2) stations (meq).

Station	Parameter	SO_4	Cl	CO_3	HCO_3	K	Na	Mg	Ca	PH	T.D.S	EC
1	SD	0.61	1.27	148.3	0.7	0.02	1.23	0.5	0.91	0.13	160.57	243.09
2		0.58	0.13	118.3	0.52	0.01	0.1	0.47	0.32	0.19	33.07	49.61
1	CV (%)	42.36	62.87	49.96	15.91	28.57	57.75	25.25	23.64	1.65	29.29	28.74
2		34.73	19.4	47.47	15.62	20	16.67	27.81	9.17	2.37	8.6	8.27
1	Median	1.3	1.4	275	4.5	0.06	1.95	2.2	3.65	7.9	506	770
2		1.6	0.6	255	3.5	0.05	0.6	1.75	3.5	7.9	381.5	593.5
1	Variance	0.37	1.62	21,989	0.5	0	1.52	0.25	0.82	0.02	25,783	59,092
2		0.34	0.02	13,983	0.27	0	0.01	0.22	0.1	0.04	1093.6	2461.5

As evident from Tables 8 and 9, the trend of water ions at Kordkhil station over the past 20 years (2001–2021) has shown a significance level of 0.05 in all parameters, except for magnesium (Mg). This decrease in the Mg parameter suggests a decline in water quality during this period.

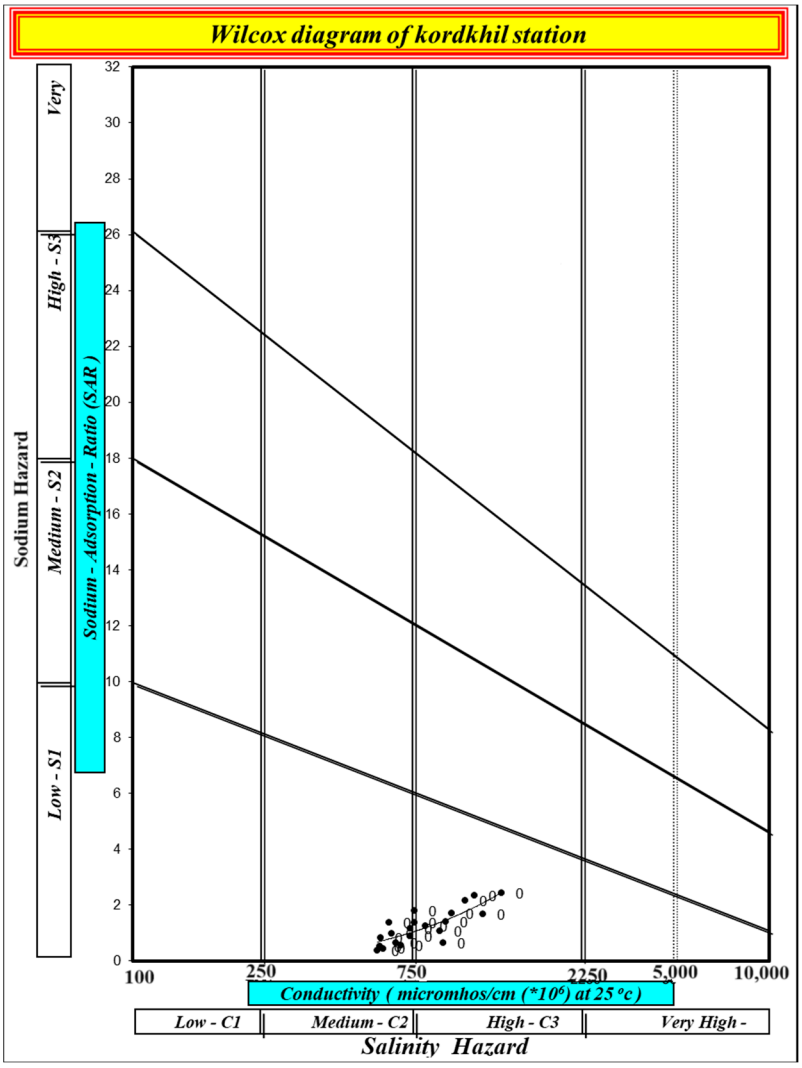

Figure 9. *Cont.*

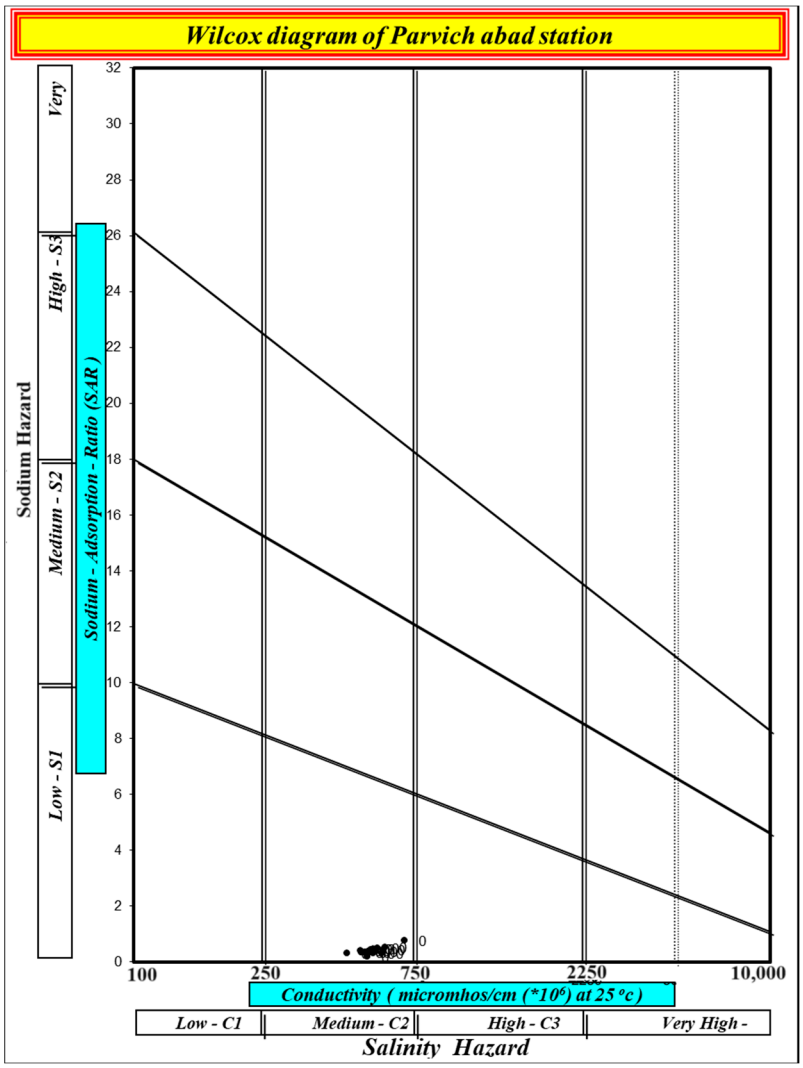

Figure 9. Agricultural water quality in Kordkhil (**top**) and Parvich abad (**down**) stations presented in Wilcox diagrams.

Table 8. Trend analysis of water quality parameters of Kordkhil station in the period 2001–2021 at the confidence level of 95%.

Parameter	Standard Deviation	*p*-Value	OLS Regression Slope	M-K Test Value	Trend
TDS	33.1	0.06	9.36	51	↑
EC	33.1	0.06	13.98	51	↑
PH	32.43	0.35	0.001	13	↑
Na	33.08	0.26	0.03	22	↑
TH	33.08	0.05	3.16	54	↑
Cl	33.02	0.01	0.08	75	↑
SO_4	33.04	0.07	0.03	49	↑
HCO_3	33.3	0.38	0.009	11	↑
Ca	33.3	0	0.01	111	↑
Mg	33.4	0.024	−0.03	−66	↓
K	32.64	0.005	0.001	85	↑

Notes: These arrows indicate the upward and downward trend.

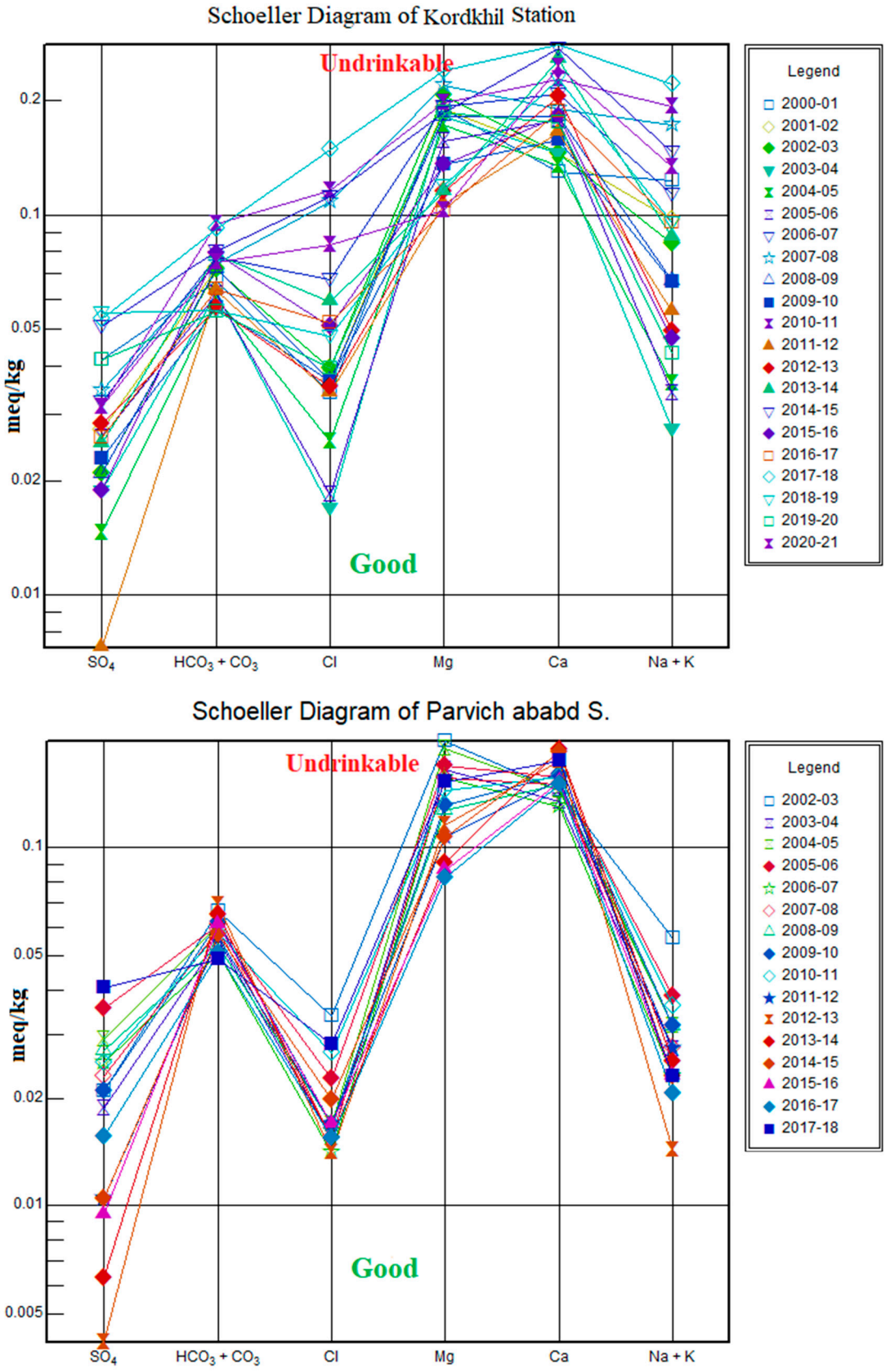

Figure 10. Drinking water quality at Kordkhil (**top**) and Parvich abad (**down**) stations presented in Schuler's diagrams.

Table 9. Trend analysis of water quality parameters of Parvich abad station in the period 2001–2021 at the confidence level of 95%.

Parameter	Standard Deviation	*p*-Value	OLS Regression Slope	M-K Test Value	Trend
TDS	22.21	0.039	−4.45	−40	↓
EC	22.21	0.032	−6.18	−42	↓
PH	21.74	0.029	0.027	42	↑*
Na	21.84	0	−0.02	−60	↓
TH	22.18	0.29	−1.55	−13	↓
Cl	21.61	0.5	−0.003	1	↓
SO_4	22.14	0.08	−0.03	−31	↓
HCO_3	22.16	0.12	−0.02	−26	↓
Ca	22.06	0	0.04	56	↑*
Mg	22.16	0	−0.08	−86	↓
K	18.01	0.06	−0.003	−28	↓

Notes: * These arrows indicate the upward and downward trend.

Because of its location at the outlet of the watershed, Kordkhil station receives water from various rivers in the upstream areas of the watershed. These rivers have different land use and formations, which results in lower water quality compared to the higher stations. Most of the land use changes and human activities are concentrated in the downstream areas of the watershed, directly impacting the water quality of this station. To compare the water quality downstream and upstream of the watershed, we also analyzed the trend of water quality at the Parvich abad station, which is located upstream of the Shahid Rajaei Dam. The results of this analysis showed that, unlike the Kordkhil station, the trend of ions in this station was decreasing in all parameters except for calcium (Ca) and pH. These results can also be attributed to the reduced influence of human activities on the water entering this station. The trend diagram of water quality parameters in Kordkhil station, as an example, is also shown in Figure 11. In addition, Figure 12 shows the trend of some water quality parameters with two types of climatic and hydrological drought. The results demonstrate the different behavior of water quality parameters and drought indices in the study area.

Figure 11. *Cont.*

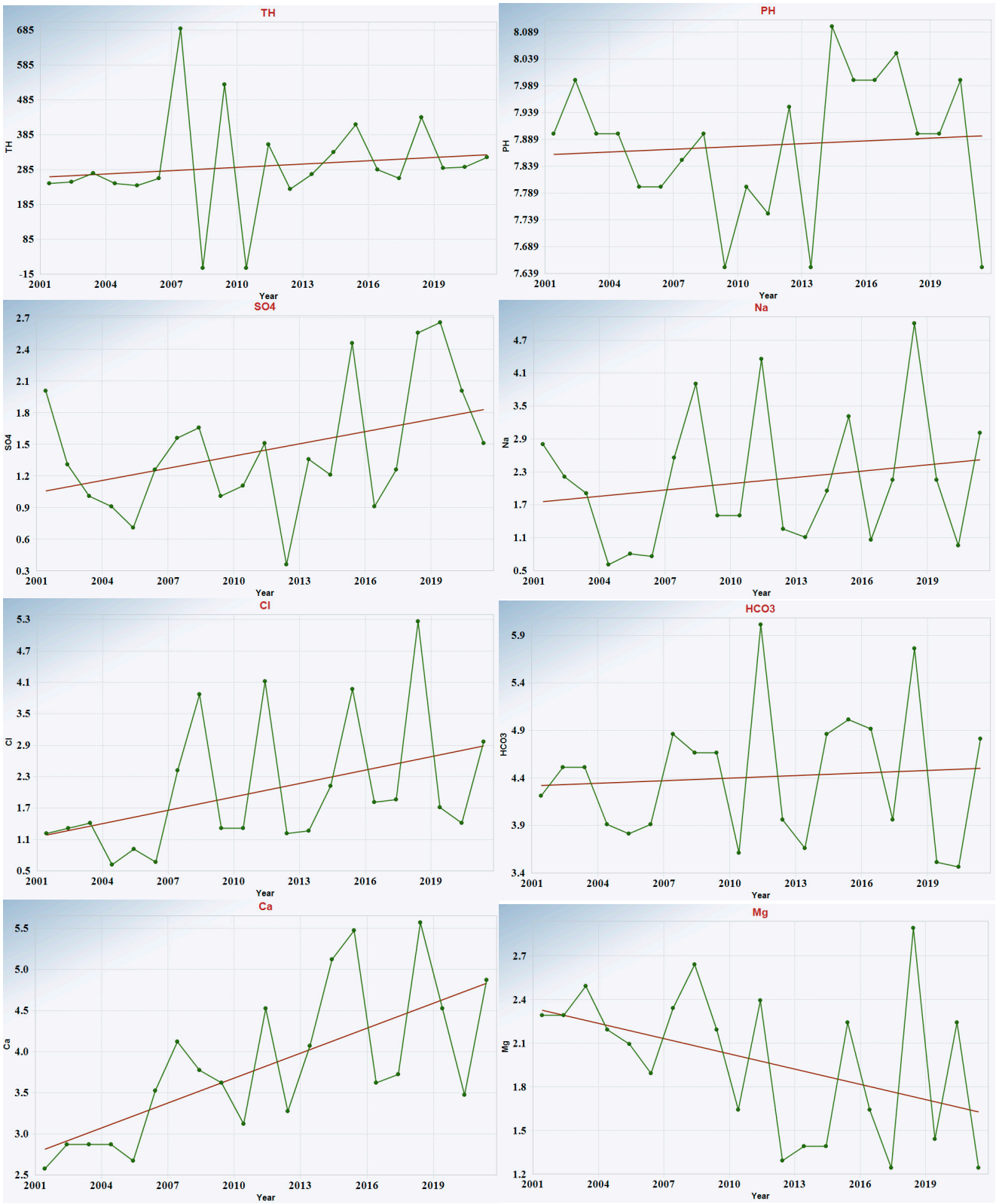

Figure 11. The trend of water quality parameters of Kordkhil station in the period 2001–2021 (Red and green lines respectively indicating the Sen's slope and Mann–Kendall trend).

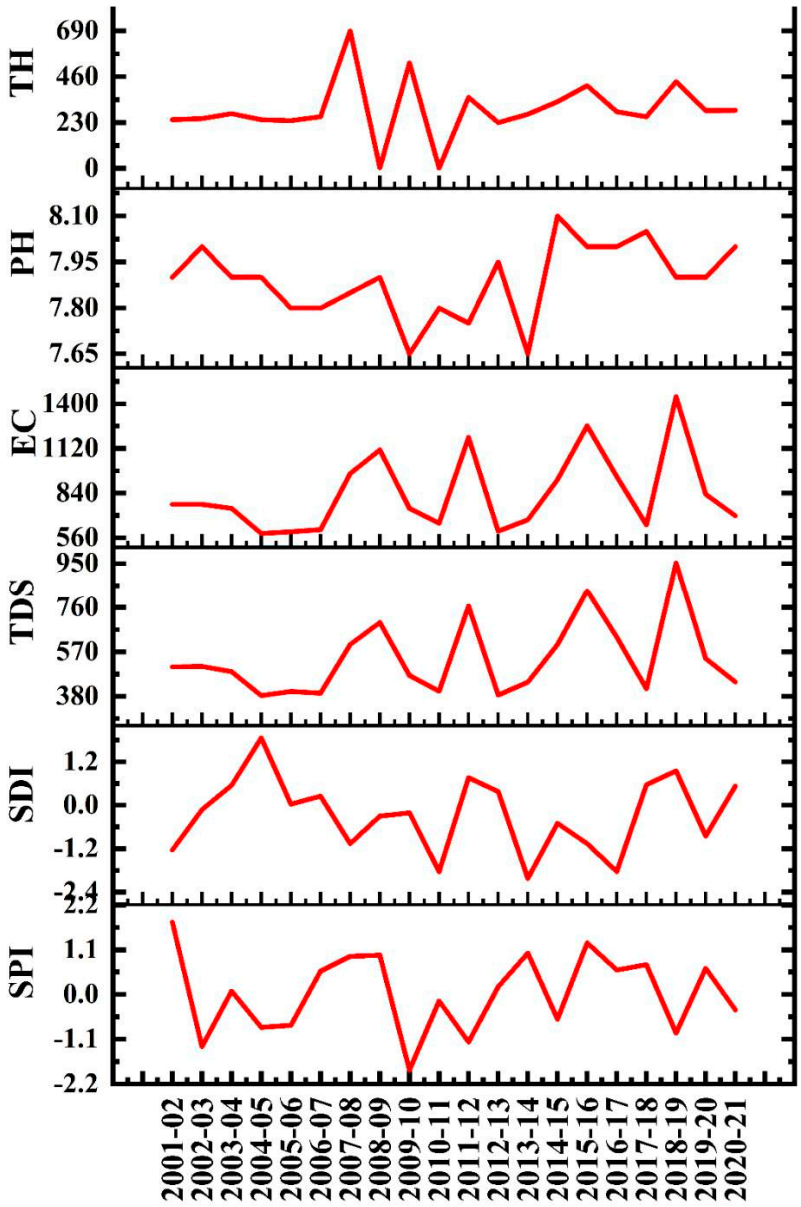

Figure 12. Simultaneous trends of some water quality parameters and drought.

3.4. Results of Land Use/Cover Changes Assessment

The study of land use changes revealed that the dominant land uses are forest, agriculture, rangeland, garden, and residential (Figure 13). The results of land use changes, based on the continuity scenario, indicate that if future changes follow the trends of the past 29 years, the area of forest lands will decrease by 19.77 km^2, which is equivalent to a 2.02% decrease in the current forest land area over the next 20 years. In this scenario, the rangeland area may decrease by −5.74%. Residential, agricultural, and garden lands are projected to increase by 0.45, 6.82, and 9.17, respectively, during this period (Figure 12, Table 10).

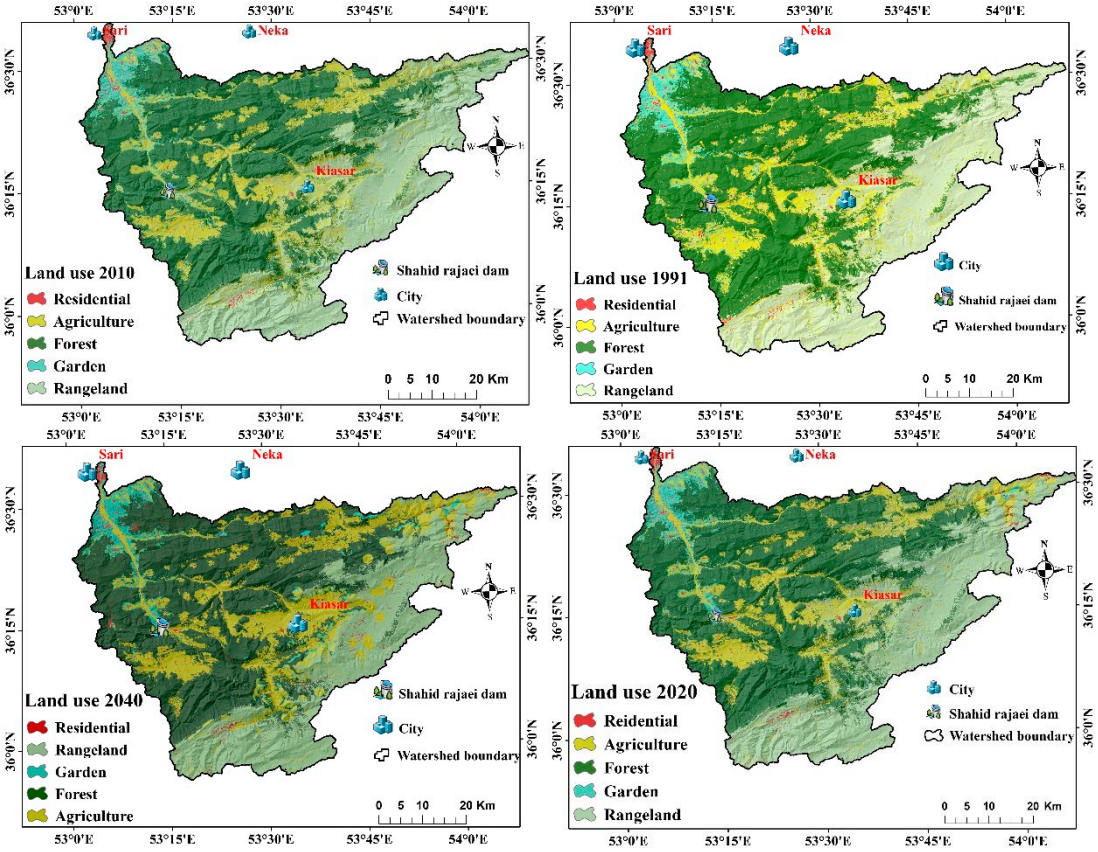

Figure 13. The trend of land use changes in the Tajan watershed in the basic and future periods.

Table 10. The difference in land use area in the two periods of 2020 and 2040.

Land Use	1991	2010	2020	2040	Difference (Km^2)	Difference (%)
Residential	32.62	43.96	47.05	64.34	17.29	0.45
Agriculture	585.17	681.84	614.54	874.75	260.21	6.82
Forest	1974.3	1872.8	1890.61	1813.42	−77.19	−2.02
Garden	145.97	177.42	152.02	187	34.98	9.17
Rangeland	1218.59	1172.17	1229.6	1010.77	−218.83	−5.74

If the current trend of land use change in the studied area continues, approximately 213.21 km^2 of rangelands and 64.84 km^2 of forests will be converted into agricultural lands by 2040 (Table 10). The least amount of change occurs when garden lands are converted into residential lands. The expansion of agricultural and residential areas, often located along riverbanks, has contributed to the increased use of chemical fertilizers and the discharge of domestic sewage into rivers, leading to environmental pollution. An increase in sediment in surface water and a decrease in water and soil quality are additional consequences of expanding agricultural and residential land, which is also demonstrated by previous research [20–22,34]. Therefore, land use management in a region can significantly impact the health of the watershed.

The results of investigating the impact of drought on NDVI in the studied watershed over a 20-year period (2000–2020) is shown in Figures 14 and 15. The results indicate a recent increase in vegetation cover, likely due to the expansion of agricultural lands or gardens in the study area. The level of agricultural and garden lands has been increasing in recent years. Despite a decrease in precipitation in recent years, the amount of greenness has not significantly decreased, except in 2021–2022 (Figures 14 and 15).

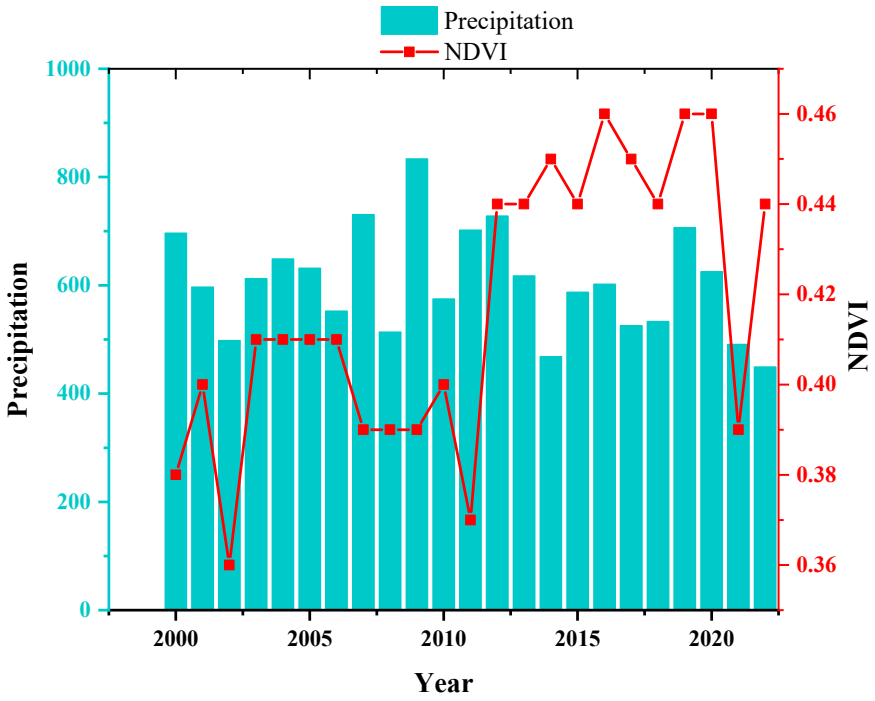

Figure 14. NDVI and precipitation (mm) trend in the period of 2000–2022.

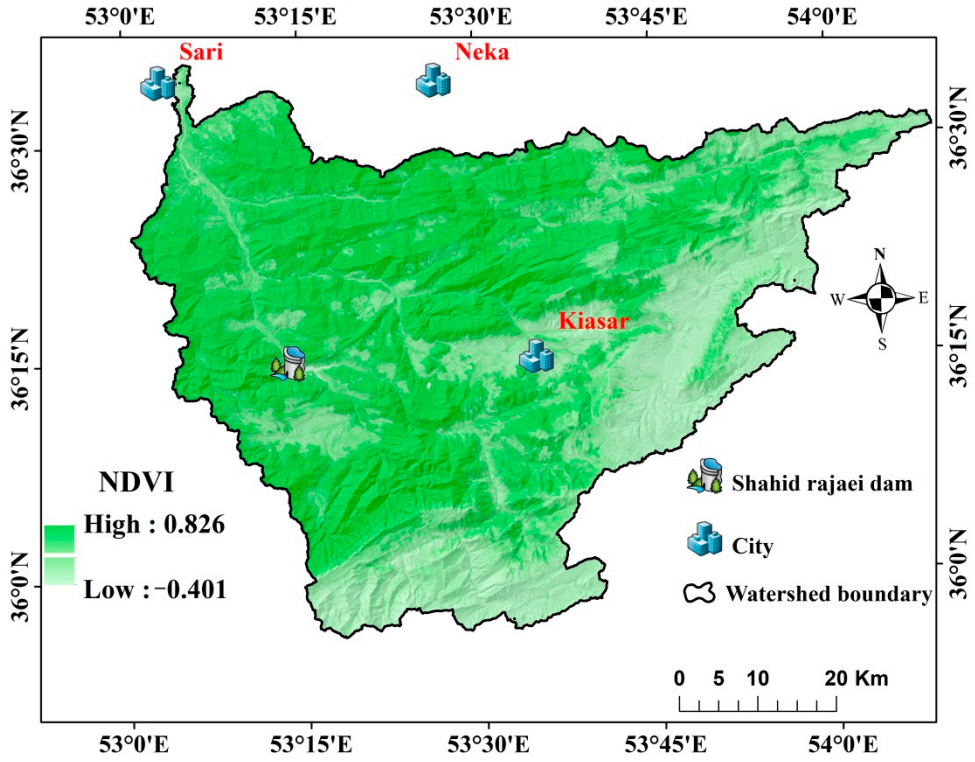

Figure 15. NDVI map of Tajan watershed in the period of 2000–2020.

The changes in the NDVI compared to the meteorological index of SPI from 2000 to 2021 in various stations clearly shows that the NDVI does not align with the SPI, particularly in recent years (Figure 16 and Table 11). It can be concluded that the drought had minimal impact on the greenness index of the Tajan watershed (Figure 16 and Table 11). This is likely because the watershed has ample surface water resources. These results contradict the findings of Zhang et al. [33] regarding the adverse impact of drought on vegetation.

Considering that the NDVI only measures vegetation, it is possible that the expansion of agricultural and garden lands during this period has led to an increase in the NDVI. Therefore, this index should be considered in conjunction with other factors when assessing the impact of drought and the overall health of the watershed. In this regard, Ji and Peters [57] reported a significant effect of seasonality on the NDVI-SPI relationship. The high correlations were obtained only in the middle of the growing season, which reflects the sensitivity to water availability in this time.

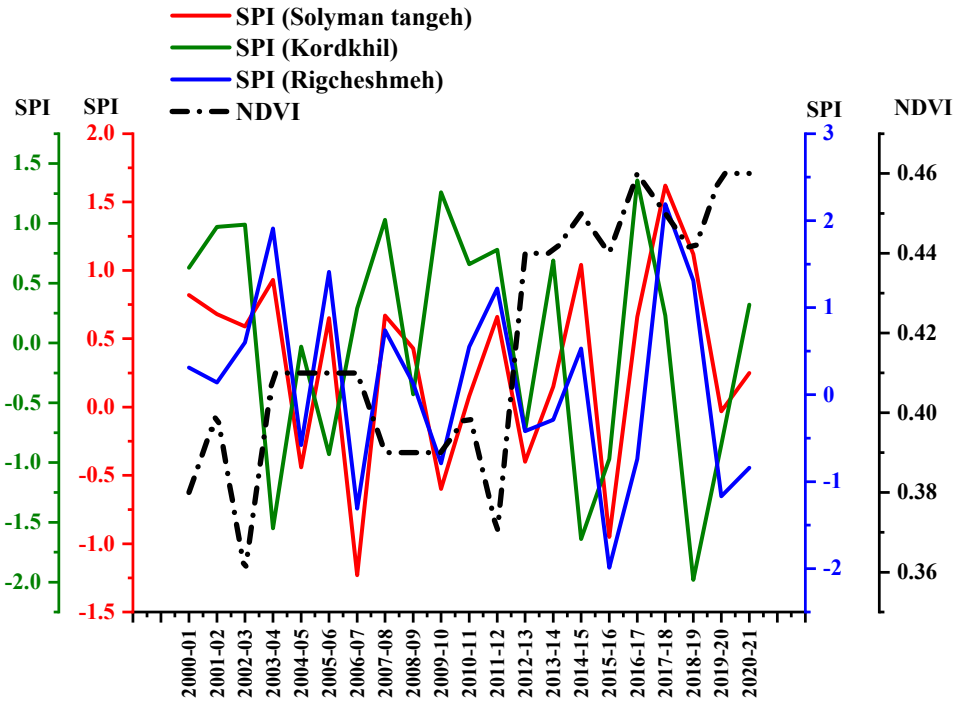

Figure 16. NDVI and SPI changes trend with a 12-month time step in different stations.

Table 11. Statistical analysis of changes in SPI and NDVI.

Index	Mean	Standard Deviation	Standard Error	Mean Absolute Deviation	Median
SPI (Soleyman tangeh)	0.319	0.718	0.156	0.575	0.59
SPI (Kordkhil)	0.004	1.02	0.222	0.871	0.29
SPI (Rigcheshmeh)	0.138	1.104	0.24	0.893	0.14
NDVI	0.417	0.031	0.006	0.027	0.41

4. Conclusions

The analysis of both climate scenarios (RCP2.6 and RCP8.5) indicates the potential for severe droughts in certain years in the future, despite the possibility of wet climate conditions in other years. In addition, the hydrological drought in the Tajan river has exhibited fluctuations, with some years experiencing a decrease in flow and others showing an increase. The results of land use analysis indicate an increase in agricultural, garden, and residential land, while forests and rangelands have decreased. Therefore, the reduction in permanent forest and rangeland cover may lead to increased runoff and flooding, resulting in higher flow rates during certain times of the year. Therefore, a drought in a region experiencing simultaneous changes in climate and land use can yield varying outcomes. The changes in NDVI did not comply with the SPI. Changes in a watershed have a significant impact on surface water quality, making it an important health factor to consider. Given the observed increase in agricultural land, particularly in rainfed areas, in the studied region, it is anticipated that without proper measures, water quality will decline

in the future. The changes mentioned above pose a threat to the health of watersheds from the standpoint of the number and intensity of floods, erosion and sedimentation, decreased water penetration into aquifers, increased pollutants, and decreased water resources.

Author Contributions: Conceptualization, M.A., H.R.M., and Z.H.; methodology, software, and data curation, M.A.; validation, M.A. and Z.H.; writing—original draft preparation, M.A.; writing—review and editing, M.A. and Z.H. All authors have read and agreed to the published version of the manuscript.

Funding: This work is based upon research funded by the Iran National Science Foundation (INSF) under project No. 4014817.

Data Availability Statement: The data will be shared upon reasonable request.

Conflicts of Interest: The authors declare no conflicts of interest.

References

1. Kumar, S.; Madhu, M.; Singh, R.K.; Kaushal, R.; Dash, C.J.; Gowda, H.H.; Barla, G. Changes in the value of ecosystem services due to watershed development in India's Eastern Ghats and incentives for better stewardship. *Ecosyst. Serv.* **2024**, *65*, 101580. [CrossRef]
2. Moghadam, N.T.; Malekmohammadi, B.; Schirmer, M. Vulnerability assessment of hydrological ecosystem services under future climate and land use change dynamics. *Ecol. Indic.* **2024**, *160*, 111905. [CrossRef]
3. Hazbavi, Z.; Sadeghi, S.H.; Gholamalifard, M.; Davudirad, A.A. Watershed health assessment using the pressure–state–response (PSR) framework. *Land Degrad. Dev.* **2019**, *31*, 3–19. [CrossRef]
4. Xue, D.; Zhou, J.; Zhao, X.; Liu, C.; Wei, W.; Yang, X.; Li, Q.; Zhao, Y. Impacts of climate change and human activities on runoff change in a typical arid watershed, NW China. *Ecol. Indic.* **2021**, *121*, 107013. [CrossRef]
5. Mo, C.; Lai, S.; Yang, Q.; Huang, K.; Lei, X.; Yang, L.; Yan, Z.; Jiang, C. A comprehensive assessment of runoff dynamics in response to climate change and human activities in a typical karst watershed, southwest China. *J. Environ. Manag.* **2023**, *332*, 117380. [CrossRef]
6. IPCC. Summary for policymakers. In *Climate Change 2023: Synthesis Report*; The Core Writing Team, Lee, H., Romero, J., Eds.; Contribution of Working Groups I, II and III to the Sixth Assessment Report of the Intergovernmental Panel on Climate Change; IPCC: Geneva, Switzerland, 2023; pp. 1–34. [CrossRef]
7. Scafetta, N. Impacts and risks of "realistic" global warming projections for the 21st century. *Geosci. Front.* **2024**, *15*, 101774. [CrossRef]
8. Hazbavi, Z.; Baartman, J.E.; Nunes, J.P.; Keesstra, S.D.; Sadeghi, S.H. Changeability of reliability, resilience and vulnerability indicators with respect to drought patterns. *Ecol. Indic.* **2018**, *87*, 196–208. [CrossRef]
9. Azizi, E.; Nikoo, M.R.; Mostafazadeh, R.; Hazbavi, Z. Flood vulnerability analysis using different aggregation frameworks across watersheds of Ardabil province, northwestern Iran. *Int. J. Disaster Risk Reduct.* **2023**, *91*, 103680. [CrossRef]
10. Afsahhosseini, F. The impact of Iran's urban heritage on sustainability, climate change and carbon zero. *Environ. Dev. Sustain.* **2024**, 1–41. [CrossRef]
11. Khoorani, A.; Balaghi, S.; Mohammadi, F. Projecting drought trends and hot spots across Iran. *Nat. Hazards* **2024**, 1–14. [CrossRef]
12. Afsari, R.; Nazari-Sharabian, M.; Hosseini, A.; Karakouzian, M. A CMIP6 multi-model analysis of the impact of climate change on severe meteorological droughts through multiple drought indices—Case study of Iran's Metropolises. *Water* **2024**, *16*, 711. [CrossRef]
13. Madani, K.; AghaKouchak, A.; Mirchi, A. Iran's socio-economic drought: Challenges of a water-bankrupt nation. *Iran. Stud.* **2016**, *49*, 997–1016. [CrossRef]
14. WMO. *Guidelines on the Definition and Monitoring of Extreme Weather and Climate Events*; Final Version Forthcoming; World Meteorological Organization (WMO): Geneva, Switzerland, 2020; Available online: https://library.wmo.int/records/item/58396-guidelines-onthe-definition-and-characterization-of-extreme-weather-and-climate-events (accessed on 29 April 2022).
15. Ghabelnezam, E.; Mostafazadeh, R.; Hazbavi, Z.; Huang, G. Hydrological drought severity in different return periods in rivers of Ardabil Province, Iran. *Sustainability* **2023**, *15*, 1993. [CrossRef]
16. CRED. *2021: Disasters in Numbers*; CRED: Brussels, Belgium, 2022; Available online: https://cred.be/sites/default/files/2021_EMDAT_report.pdf (accessed on 29 April 2022).
17. Stefanidis, S.; Rossiou, D.; Proutsos, N. Drought severity and trends in a Mediterranean oak forest. *Hydrology* **2023**, *10*, 167. [CrossRef]
18. Wei, W.; Liu, T.; Zhou, L.; Wang, J.; Yan, P.; Xie, B.; Zhou, J. Drought-related spatiotemporal cumulative and time-lag effects on terrestrial vegetation across China. *Remote. Sens.* **2023**, *15*, 4362. [CrossRef]
19. Kazemzadeh, M.; Malekian, A. Changeability evaluation of hydro-climate variables in Western Caspian Sea region, Iran. *Environ. Earth Sci.* **2018**, *77*, 120. [CrossRef]
20. Luo, Z.; Shao, Q.; Zuo, Q.; Cui, Y. Impact of land use and urbanization on river water quality and ecology in a dam dominated basin. *J. Hydrol.* **2020**, *584*, 124655. [CrossRef]

21. Shi, P.; Zhang, Y.; Li, Z.; Li, P.; Xu, G. Influence of land use and land cover patterns on seasonal water quality at multi-spatial scales. *Catena* **2017**, *151*, 182–190. [CrossRef]
22. Ding, J.; Jiang, Y.; Fu, L.; Liu, Q.; Peng, Q.; Kang, M. Impacts of land use on surface water quality in a subtropical River Basin: A case study of the Dongjiang River Basin, Southeastern China. *Water* **2015**, *7*, 4427–4445. [CrossRef]
23. Moradzadeh, V.; Hazbavi, Z.; Ouri, A.E.; Mostafazadeh, R.; Rodrigo-Comino, J.; Zareie, S.; Fernández-Raga, M. A Multifunctional conceptual framework for ecological disturbance assessment. *Earth Syst. Environ.* **2024**, 1–19. [CrossRef]
24. Alamdari, N.; Claggett, P.; Sample, D.J.; Easton, Z.M.; Yazdi, M.N. Evaluating the joint effects of climate and land use change on runoff and pollutant loading in a rapidly developing watershed. *J. Clean. Prod.* **2022**, *330*, 129953. [CrossRef]
25. Mishra, A.; Alnahit, A.; Campbell, B. Impact of land uses, drought, flood, wildfire, and cascading events on water quality and microbial communities: A review and analysis. *J. Hydrol.* **2020**, *596*, 125707. [CrossRef]
26. Gong, L.; Zhang, X.; Pan, G.; Zhao, J.; Zhao, Y. Hydrological responses to co-impacts of climate change and land use/cover change based on CMIP6 in the Ganjiang River, Poyang Lake basin. *Anthropocene* **2023**, *41*, 100368. [CrossRef]
27. Ahmadi, A.; Jalali, J.; Mohammadpour, A. Future runoff assessment under climate change and land-cover alteration scenarios: A case study of the Zayandeh-Roud dam upstream watershed. *Hydrol. Res.* **2022**, *53*, 1372–1392. [CrossRef]
28. Ahmed, N.; Wang, G.; Booij, M.J.; Xiangyang, S.; Hussain, F.; Nabi, G. Separation of the impact of landuse/landcover change and climate change on runoff in the upstream area of the Yangtze River, China. *Water Resour. Manag.* **2022**, *36*, 181–201. [CrossRef]
29. Chang, D.; Li, S.; Lai, Z.; Fu, F.; Qi, X. Integrated effects of co-evolutions among climate, land use and vegetation growing dynamics to changes of runoff quantity and quality. *J. Environ. Manag.* **2023**, *331*, 117195. [CrossRef]
30. Haleem, K.; Khan, A.U.; Ahmad, S.; Khan, M.; Khan, F.A.; Khan, W.; Khan, J. Hydrological impacts of climate and land-use change on flow regime variations in upper Indus basin. *J. Water Clim. Change* **2022**, *13*, 758–770. [CrossRef]
31. Sabitha, N.M.; Thampi, S.G.; Kumar, D.S. Application of a distributed hydrologic model to assess the impact of climate and land-use change on Surface Runoff from a small urbanizing Watershed. *Water Resour. Manag.* **2023**, *37*, 2347–2368. [CrossRef]
32. Shahid, M.; Rahman, K.U.; Haider, S.; Gabriel, H.F.; Khan, A.J.; Pham, Q.B.; Pande, C.B.; Linh, N.T.T.; Anh, D.T. Quantitative assessment of regional land use and climate change impact on runoff across Gilgit watershed. *Environ. Earth Sci.* **2021**, *80*, 743. [CrossRef]
33. Zhang, H.; Meng, C.; Wang, Y.; Wang, Y.; Li, M. Comprehensive evaluation of the effects of climate change and land use and land cover change variables on runoff and sediment discharge. *Sci. Total. Environ.* **2020**, *702*, 134401. [CrossRef]
34. de Mello, K.; Taniwaki, R.H.; de Paula, F.R.; Valente, R.A.; Randhir, T.O.; Macedo, D.R.; Leal, C.G.; Rodrigues, C.B.; Hughes, R.M. Multiscale land use impacts on water quality: Assessment, planning, and future perspectives in Brazil. *J. Environ. Manag.* **2020**, *270*, 110879. [CrossRef] [PubMed]
35. Gani, M.A.; Sajib, A.M.; Siddik, M.A.; Moniruzzaman, M. Assessing the impact of land use and land cover on river water quality using water quality index and remote sensing techniques. *Environ. Monit. Assess.* **2023**, *195*, 449. [CrossRef]
36. Gu, Q.; Hu, H.; Ma, L.; Sheng, L.; Yang, S.; Zhang, X.; Zhang, M.; Zheng, K.; Chen, L. Characterizing the spatial variations of the relationship between land use and surface water quality using self-organizing map approach. *Ecol. Indic.* **2019**, *102*, 633–643. [CrossRef]
37. Sadeghi, S.H.; Vafakhah, M.; Moosavi, V.; Asadabadi, S.P.; Sadeghi, P.S.; Darvishan, A.K.; Fahraji, R.B.; Mosavinia, S.H.; Majidnia, A.; Gharemahmudli, S.; et al. Interactive impacts of climatic, hydrologic, and anthropogenic activities on watershed health. *Sci. Total Environ.* **2019**, *648*, 880–893. [CrossRef]
38. Wan, R.; Cai, S.; Li, H.; Yang, G.; Li, Z.; Nie, X. Inferring land use and land cover impact on stream water quality using a Bayesian hierarchical modeling approach in the Xitiaoxi River Watershed, China. *J. Environ. Manag.* **2014**, *133*, 1–11. [CrossRef] [PubMed]
39. Yao, S.; Chen, C.; He, M.; Cui, Z.; Mo, K.; Pang, R.; Chen, Q. Land use as an important indicator for water quality prediction in a region under rapid urbanization. *Ecol. Indic.* **2023**, *146*, 109768. [CrossRef]
40. Khadka, D.; Babel, M.S.; Tingsanchali, T.; Penny, J.; Djordjevic, S.; Abatan, A.A.; Giardino, A. Evaluating the impacts of climate change and land-use change on future droughts in northeast Thailand. *Sci. Rep.* **2024**, *14*, 9746. [CrossRef]
41. Peña-Guerrero, M.D.; Nauditt, A.; Muñoz-Robles, C.; Ribbe, L.; Meza, F. Drought impacts on water quality and potential implications for agricultural production in the Maipo River Basin, Central Chile. *Hydrol. Sci. J.* **2020**, *65*, 1005–1021. [CrossRef]
42. Avand, M.; Moradi, H.; Lasboyee, M.R. Spatial modeling of flood probability using geo-environmental variables and machine learning models, case study: Tajan watershed, Iran. *Adv. Space Res.* **2021**, *67*, 3169–3186. [CrossRef]
43. Tavangar, S.; Moradi, H.; Massah Bavani, A.R. Climate change effect on the rainfall amount and intensity in the southern coast of the Caspian Sea. *Irrig. Water Eng.* **2019**, *10*, 190–204.
44. Semenov, M.A.; Barrow, E.M. *LARS-WG: A Stochastic Weather Generator for Use in Climate Impact Studies, User Manual*; Version 3.0, Herts, UK; 2002; pp. 1–27. Available online: http://resources.rothamsted.ac.uk/sites/default/files/groups/mas-models/download/LARS-WG-Manual.pdf (accessed on 29 April 2022).
45. McKee, T.B.N.; Doesken, J.; Kliest, J. The relationship of drought frequency and duration to time scales. In Proceedings of the 8th Conference on Applied Climatology, Anaheim, CA, USA, 17–22 January 1993; American Meteorological Society: Washington, DC, USA, 1993. 6p.
46. Jang, D. Assessment of meteorological drought indices in Korea using RCP 8.5 scenario. *Water* **2018**, *10*, 283. [CrossRef]
47. Nalbantis, I. Evaluation of a hydrological drought index. *Eur. Water* **2008**, *23*, 67–77.

48. Hong, X.; Guo, S.; Zhou, Y.; Xiong, L. Uncertainties in assessing hydrological drought using streamflow drought index for the upper Yangtze River basin. *Stoch. Environ. Res. Risk Assess.* **2015**, *29*, 1235–1247. [CrossRef]
49. Jakeman, A.J.; Littlewood, I.G.; Whitehead, P.G. Computation of the instantaneous unit hydrograph and identifiable component flows with application to two small upland catchments. *J. Hydrol.* **1990**, *117*, 275–300. [CrossRef]
50. Croke, B.F.W.; Jakeman, A.J. Use of the IHACRES rainfall-runoff model in arid and semi arid regions. In *Hydrological Modelling in Arid and Semi-Arid Areas*; International Hydrology Series, Weather, H., Soroshian, S., Sharma, K.D., Eds.; Cambridge University Press: Cambridge, UK, 2008; pp. 41–48.
51. Mohammadi, B.; Safari, M.J.S.; Vazifehkhah, S. IHACRES, GR4J and MISD-based multi conceptual-machine learning approach for rainfall-runoff modeling. *Sci. Rep.* **2022**, *12*, 12096. [CrossRef] [PubMed]
52. Dodangeh, E.; Shahedi, K.; Soleimani, K. Application of Copula theory for IHACRES hydrologic model evaluation (Case study: Taleghan watershed). *J. Earth Space Phys.* **2018**, *44*, 71–88. [CrossRef]
53. Mann, H.B. Non-parametric tests against trend. *Econometrica* **1945**, *13*, 245–259. [CrossRef]
54. Kendall, M.G. *Rank Correlation Methods*, 4th ed.; Charles Griffin: London, UK, 1975.
55. Todman, J.; Dugard, R. *Approaching Multivariate Analysis: A Guide for Psychology*; Psychological Press: Hove, UK, 2007.
56. Abijith, D.; Saravanan, S. Assessment of land use and land cover change detection and prediction using remote sensing and CA Markov in the northern coastal districts of Tamil Nadu, India. *Environ. Sci. Pollut. Res.* **2022**, *29*, 86055–86067. [CrossRef]
57. Ji, L.; Peters, A.J. Assessing vegetation response to drought in the northern Great Plains using vegetation and drought indices. *Remote. Sens. Environ.* **2003**, *87*, 85–98. [CrossRef]
58. Lin, C.Y. A study on the width and placement of vegetated buffer strips in a mudstone-distributed watershed. *J. Chin. Soil Water Conserv.* **1997**, *29*, 250–266. (In Chinese with English abstract)
59. Tramblay, Y.; El Khalki, E.M.; Ciabatta, L.; Camici, S.; Hanich, L.; Saidi, M.E.M.; Ezzahouani, A.; Benaabidate, L.; Mahé, G.; Brocca, L. River runoff estimation with satellite rainfall in Morocco. *Hydrol. Sci. J.* **2023**, *68*, 474–487. [CrossRef]